Plasmonics
DOI 10.1007/s11468-015-9986-2

High Performance Broadband Asymmetric Polarization Conversion Due to Polarization-dependent Reflection

Zhancheng Li[1] · Shuqi Chen[1] · Wenwei Liu[1] · Hua Cheng[1] · Zhaocheng Liu[1] · Jianxiong Li[1] · Ping Yu[1] · Boyang Xie[1] · Jianguo Tian[1]

Received: 11 March 2015 / Accepted: 8 May 2015

Abstract We present the underlying theory, the design specifications, and the simulated demonstration of a high performance broadband asymmetric polarization conversion composed of an L-shaped gold particle and a gold nanoantenna array for the near-infrared regime. It can transform linearly polarized light to its cross polarization in the transmission mode for one propagation direction and efficiently reflect the light for the opposite propagation direction. The broadband asymmetric polarization conversion can be attributed to the polarization-dependent reflection of the nanoantenna array, which enhances the polarization conversion efficiency of the L-shaped particle and makes it asymmetric and devisable. This work offers a further step in the development of a high efficiency broadband optical activity device.

Keywords Metamaterials · Surface plasmons · Polarization

✉ Shuqi Chen
schen@nankai.edu.cn

✉ Hua Cheng
hcheng@nankai.edu.cn

✉ Jianguo Tian
jjtian@nankai.edu.cn

[1] The Key Laboratory of Weak Light Nonlinear Photonics, Ministry of Education, School of Physics and Teda Applied Physics Institute, Nankai University, Tianjin 300071, China

Introduction

Harnessing light for modern photonic applications involves very often the control and manipulation of light polarization. The ability to control the polarization of light is a fundamental desire for people to fully control light, which has great importance for practical applications such as photography, liquid crystal displays, fiber communication, sensing, and so on [1, 2]. Traditional approaches to controlling the light polarization employ the combinations of linear polarizers and dielectric wave plates. However, there exist some inherent disadvantages in the size and collimation of these systems, resulting in difficulties in optical system miniaturization and integration. Recently, realization of polarization conversion by plasmonic metasurfaces or metamaterial has attracted growing attention in the scientific community. This effect is similar to Faraday rotation but requires no magnetic field or nonreciprocal materials. Remarkable progresses have been shown in the GHz [3–5], infrared [6–8], and optical frequencies [9, 10]. A cross polarization rotator with high efficiency has been realized in GHz by a bilayered chiral metamaterials with enantiomeric patterns of fourfold rotational symmetry [4]. A cavity-involved plasmonic metamaterial has been proposed to realize an almost complete and efficient polarization conversion in transmissions for certain linearly polarized light in near-infrared region [6]. A near-infrared quarter-wave plate has been used to achieve a broadband circular-to-linear polarized light conversion by tailoring the dispersive properties of an array of orthogonally coupled nanodipole elements [10]. Most of these progresses rely on well-known structures: the split ring, the nanorods, the crossed nanodipoles, the L-shaped

Published online: 29 May 2015

and S-shaped metallic nanoparticles, and apertures. However, these designs always suffer from large optical loss and narrow optical response, resulting in low efficiency and limited bandwidth which separate them from the practical applications.

Thus far, much effort has been devoted to enhance the efficiency of polarization conversion and broaden the response frequency range [11–18]. An ultrathin multilayer stacked system containing twisted complementary split-ring resonators is proposed for manipulating the linear polarization of electromagnetic waves and providing asymmetric transmission in a wide GHz frequency range [11]. Broadband and highly efficient metamaterial-based polarization converters have been realized in THz recently, which rotate a linear polarization state into its orthogonal one [13]. Additionally, a wideband and efficient linear polarization conversion based on plasmonic planar antenna has been realized in mid-infrared [14]. However, these designs provide different physical mechanisms for the achievement of a similar broadband and efficient polarization conversion in different wavebands and do not establish a brief and systematic design methodology for the achievement of high performance broadband polarization conversion. Moreover, the achievement of the asymmetric polarization conversion is required for extreme polarization control, and it is also important for some applications on photonic systems. Meanwhile, an effective method to regulate the polarization conversion performance of the pre-existing designs is highly desirable.

In this paper, we present the underlying theory, the design specifications, and the simulated demonstration of a high performance broadband asymmetric polarization conversion composed of an L-shaped gold particle and a gold nanoantenna array in the near-infrared regime. A 1000-nm-wide asymmetric polarization conversion for certain linearly polarized incident wave is achieved with polarization conversion rate (PCR) more than 0.95. We demonstrate that by using a nanoantenna array with polarization-dependent reflection effect, we can not only regulate the polarization conversion performance of the L-shaped particle but also achieve an asymmetric and broadband one.

Theoretical Analysis

Let us first consider the theoretical analysis of the high performance asymmetric polarization conversion for a linearly polarized light. The transmission of coherent light through any dispersive optical system can be described by means of complex Jones matrices **T** [19, 20]. For an incoming x-polarized plane wave propagating along the $+z$ direction, its electric field can be described as:

$$\mathbf{E}_i(\mathbf{r}, t) = \begin{pmatrix} I_x \\ 0 \end{pmatrix} e^{i(kz-\omega t)}, \tag{1}$$

where ω, k, and I_x represent the frequency, wave vector, and complex amplitudes, respectively. The transmitted field is then given by

$$\mathbf{E}_t(\mathbf{r}, t) = \begin{pmatrix} T_x \\ T_y \end{pmatrix} e^{i(kz-\omega t)}. \tag{2}$$

The general complex amplitudes of the incident field to the complex amplitudes of the transmitted field can be related by **T** matrix.

$$\begin{pmatrix} T_x \\ T_y \end{pmatrix} = \begin{pmatrix} T_{xx} & T_{xy} \\ T_{yx} & T_{yy} \end{pmatrix} \begin{pmatrix} I_x \\ 0 \end{pmatrix} = \mathbf{T}^f_{lin} \begin{pmatrix} I_x \\ 0 \end{pmatrix}, \tag{3}$$

The superscript f and subscript lin indicate the forward propagation (along $+z$ direction) and a special linear base, respectively. If the medium does not contain magneto-optical material, the reciprocity theorem can be applied and the transmission matrix $\mathbf{T^b}$ for propagation in the backward direction (along $-z$ direction) can be written as:

$$\mathbf{T}^b_{lin} = \begin{pmatrix} T_{xx} & -T_{yx} \\ -T_{xy} & T_{yy} \end{pmatrix}. \tag{4}$$

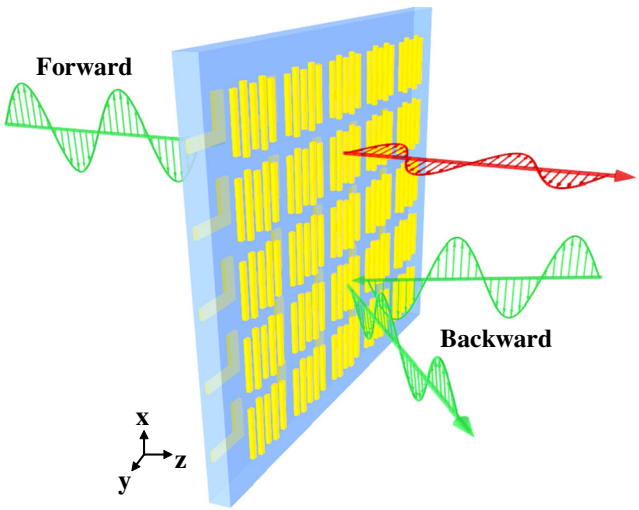

Fig. 1 An artistic rendering of the asymmetric polarization conversion for the designed ultrathin hybrid metamaterial. The linearly polarized light for the forward and backward propagation can be transformed to its cross polarization and efficiently reflected, respectively

So the relative transmitted intensity for forward and backward propagation can be derived as:

$$t^f = |T_x|^2 + |T_y|^2 = (|T_{xx}|^2 + |T_{yx}|^2) \cdot |I_x|^2. \quad (5a)$$

$$t^b = |T_x|^2 + |T_y|^2 = (|T_{xx}|^2 + |T_{xy}|^2) \cdot |I_x|^2. \quad (5b)$$

PCR is introduced as:

$$PCR = \frac{t_{yx}}{t_{xx} + t_{yx}}, \quad (6)$$

which is widely used to evaluate the performance of polarization conversion. $t_{ij} = |T_{ij}|^2$ is the squared moduli of transmission matrix elements. Obviously, the effect of polarization conversion depends on the transmission matrix elements $|T_{xx}|$ and $|T_{yx}|$. If the $|T_{xx}|$ and $|T_{xy}|$ equal to 0, then the transmitted intensity can be derived as:

$$t^f = |T_x|^2 + |T_y|^2 = |T_{yx}|^2 \cdot |I_x|^2. \quad (7a)$$

$$t^b = |T_x|^2 + |T_y|^2 = 0. \quad (7b)$$

For this condition, it is obvious that the polarization conversion is only achieved for forward propagation with a PCR equal to 1. Moreover, this condition can be easily realized by combination of arbitrary polarization conversion devices and a nanoantenna array with polarization-dependent reflection. It is worth mentioning that certain linearly polarized incident wave can be almost completely reflected by the nanoantenna array and has a phase difference almost equal to π with the incident wave. In this case, the distribution of the electric field magnitude in propagating direction will be changed, which can be used to control the interaction between the

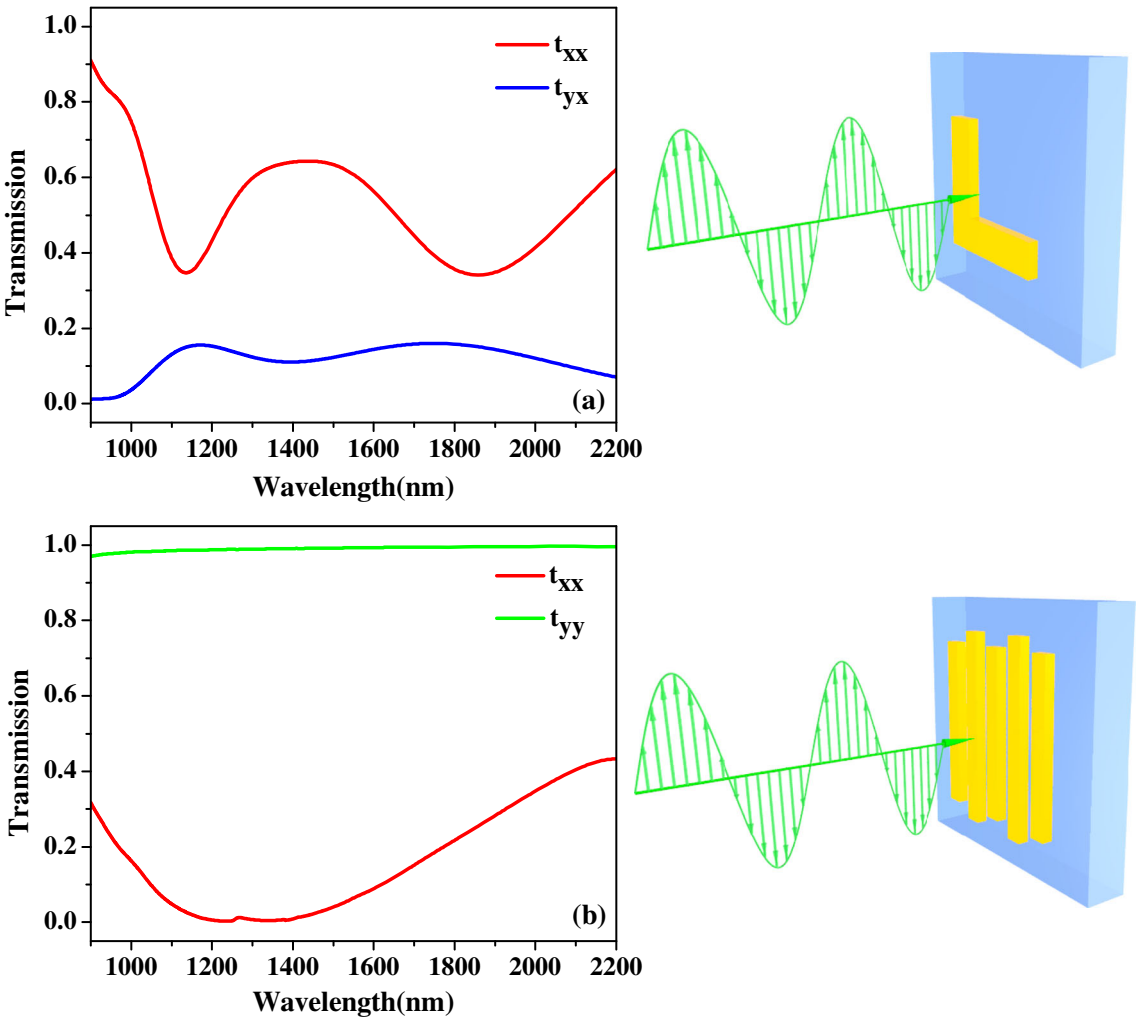

Fig. 2 The squared moduli $t_{ij} = |T_{ij}|^2$ of the T matrix of **a** the L-shaped particle and **b** the nanoantenna array

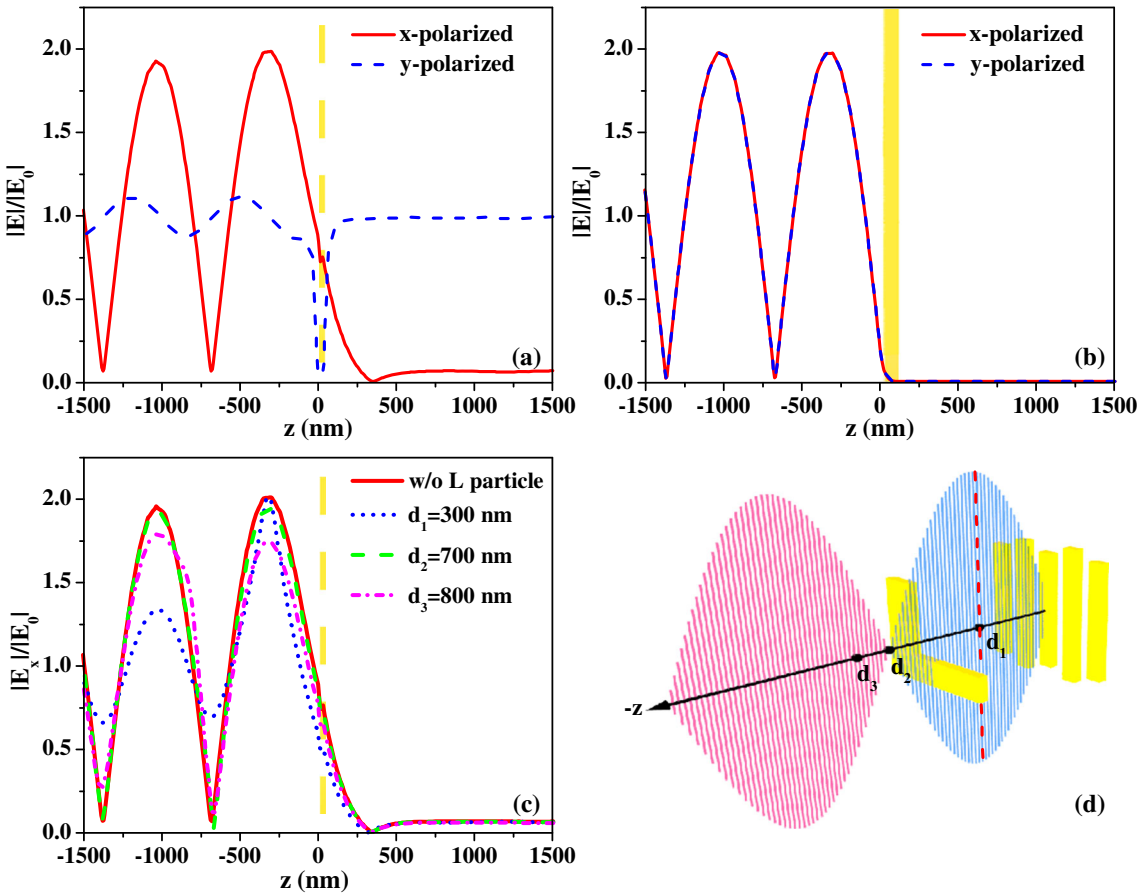

Fig. 3 Electric field profile across **a** the nanoantenna array or **b** a smooth gold mirror at 1400 nm wavelength for *x*-polarized and y-polarized incident wave. **c** $|E_x|/|E_0|$ of the nanoantenna array with or without the L-shaped particle in different position *z* for 1400 nm incident wavelength. **d** An artistic rendering of the *x*-polarized electric field magnitude distribution. The L-shaped particle can be set in different positions

polarization conversion devices and the incident wave. A broadband asymmetric polarization conversion can be further realized by setting the $|T_{yx}|$ as a constant for the designed waveband.

Design and Characteristics

To satisfy the above-mentioned condition and achieve a high performance broadband asymmetric polarization conversion, we designed an ultrathin hybrid metamaterial composed of an L-shaped gold particle and a gold nanoantenna array. Figure 1 is an artistic rendering of the asymmetric polarization conversion, which transmits the *x*-polarized wave into the opposite polarization for forward propagation and completely reflects the wave for backward propagation. The periods of the two-layer unit-cell were all $P = 650$ nm in the x and y directions. The L-shaped particle designed 380 nm in length (L_1) and 100 nm in width (W_1). The nanoantenna array designed 480 and 550 nm in length (L_2 and L_3) and 50 nm in width (W_2 and W_3), while the distance between two nanoantenna with different lengths was $s = 50$ nm. The thickness of two gold nanostructures was $t_1 = 30$ nm, and the thickness of the dielectric spacer between them was $t_2 = 300$ nm.

In order to study this ultrathin hybrid metamaterial, we have conducted numerical simulations, which were carried out by using CST microwave studio [21]. In our simulations, the dielectric function of gold is defined by Drude mode with plasmon frequency $\omega_p = 1.37 \times 10^{16}\mathrm{s}^{-1}$ and damping constant $\gamma = 4.08 \times 10^{13}\mathrm{s}^{-1}$ [22]. To account for surface scattering, grain boundary effects in the thin gold film and inhomogeneous broadening, we used a three times higher damping constant than bulk [23, 24]. We firstly do not con-

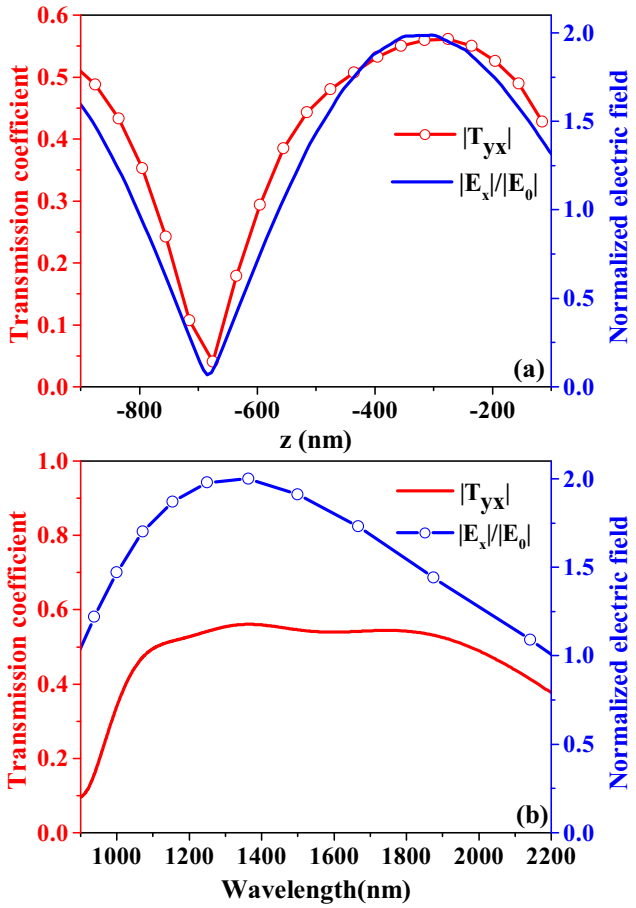

Fig. 4 **a** $|E_x|/|E_0|$ of the solitary nanoantenna array as a function of the position z for 1400 nm incident wavelength and $|T_{yx}|$ of the ultrathin hybrid metamaterial when put the L-shaped particle in the corresponding position. **b** $|E_x|/|E_0|$ of the solitary nanoantenna array and $|T_{yx}|$ of the ultrathin hybrid metamaterial for the different wavelengths when the L-shaped particle is located at 300 nm in -z direction

sider the presence of the dielectric spacer and substrate in our design (the permittivity of the dielectric is 1), which may be required in its practical realization. We will further consider its effects in the following discussion. Periodic boundary conditions were set in x and y directions representing a periodical structure, and open (perfectly matching layer) boundary is defined in z direction for the light incidence and transmission, while the excitation source is an x-polarized plane wave.

To study the polarization conversion effect of the ultrathin hybrid metamaterial in transmission mode for x-polarized incident wave, we firstly calculated the t_{ij} of the L-shaped particle and the nanoantenna array in Fig. 2, respectively. Figure 2a shows the t_{xx} and t_{yx} of the L-shaped particle. The L-shaped particle has an apparent polarization conversion effect in transmission mode, where the t_{yx} is unequal to 0 from 1000 to 2000 nm wavelength. However, the t_{yx} is much smaller than t_{xx} for a fixed wavelength, which means the polarization conversion efficiency of the L-shaped particle is pretty low. Figure 2b shows the t_{xx} and t_{yy} of the nanoantenna array. The t_{yx} and t_{xy} are equal to 0 since the nanoantenna array has no polarization conversion effect. The t_{yy} is almost equal to 1 and t_{xx} is changed from 0 to 0.4 with the variety of the wavelength. As t_{xx} is quite smaller than t_{yy} for a fixed wavelength, the reflection of nanoantenna array can be treated as polarization-dependence, which means x-polarized incident wave will be almost completely reflected and the transmitted wave is y-polarized.

To show the polarization-dependent reflection of the nanoantenna array, the electric field profile across the nanoantenna array (thickness 30 nm, center position $z = 15$ nm) or a smooth gold mirror (thickness 100 nm, center position $z = 50$ nm) for 1400 nm wavelength is showed in Figs. 3a, b. For x-polarized incident wave, the effect of the nanoantenna array is almost the same as a smooth gold mirror [25]. The incident wave is almost completely reflected. The magnitude of the electric field near the nanoantenna array becomes a function of the position z.

For y-polarized incident wave, the effect of the nanoantenna array is quite different from the gold mirror. The incident wave transmits it mostly instead of reflecting back. Basing on the polarization-dependent reflection and combining the nanoantenna array and the L-shaped particle, the polarization in transmission for the ultrathin hybrid metamaterial is orthogonal with the x-polarized incident wave. The normalized electric field distributions $|E_x|/|E_0|$ of the nanoantenna array with or without the L-shaped particle in different position z (see Fig. 3d) for 1400 nm incident wavelength are showed in Fig. 3c. The corresponding positions for the maximum and the minimum electric field magnitude have a good consistency. The difference between the distributions of $|E_x|/|E_0|$ is mainly caused by the different interaction strength between the L-shaped particle and the incident wave. The distributions of $|E_x|/|E_0|$ are quite different between the solitary nanoantenna array and the ultrathin hybrid metamaterial with the L-shaped particle in the position of the maximum electric field magnitude ($d_1 = 300$ nm), because the interaction between the L-shaped particle and the incident wave is powerful and the x-polarized electric field is largely consumed away. Since the interaction between the L-shaped particle and the incident wave is almost zero, the distributions of $|E_x|/|E_0|$ is exactly similar between the solitary nanoantenna array and the ultrathin hybrid metamaterial with the L-shaped parti-

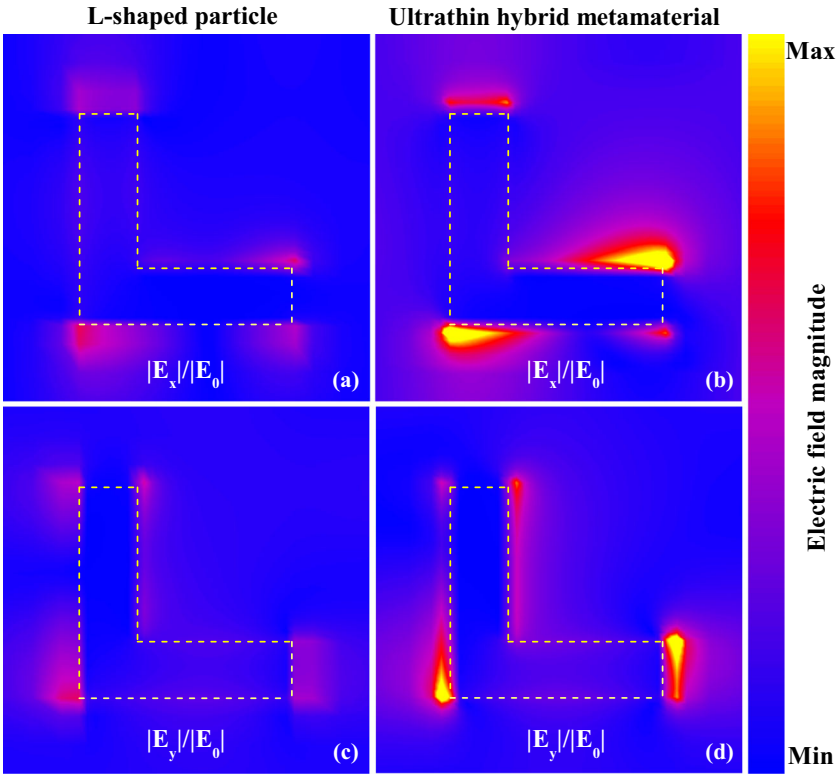

Fig. 5 Maps of the normalized electric field intensity components **a** and **b** $|E_x|/|E_0|$, **c** and **d** $|E_y|/|E_0|$ on the surface of L-shaped particle along x and y axis for **a** and **c** solitary L-shaped particle, **b** and **d** ultrathin hybrid metamaterial, where the wavelength of the incident wave is 1400 nm

cle in the position of the minimum electric field magnitude (d_2 = 700 nm). Thus, the interaction between the L-shaped particle and the incident light can be controlled by adjusting the distance between them.

When the distance between the nanoantenna array and the L-shaped particle is far enough, this system will be endowed with more physics and much different from the coupled one. For the system without existing nonlinear effect, the t_{yx} of the L-shaped particle is invariable with an increasing magnitude of the incident intensity. On the other hand, the transmitted intensity for y-polarized wave has a linear relation with the intensity of the x-polarized incident wave. It has been well established that oscillating electric current can be excited on a metallic surface upon the surrounding electromagnetic field. The surrounding electromagnetic field is then modulated by the irradiation of oscillating surface electric current. The relation between the incident intensity I and the magnitude of the electric field $|E|$ is $I \propto |E|^2$, so the t_{yx} will be changed with the magnitude variation of the electric field surrounding the L-shaped particle for a fixed incident intensity. Figure 4a shows the normalized electric field profile $|E_x|/|E_0|$ of the solitary nanoantenna array as a function of the position z for 1400 nm incident wavelength and the $|T_{yx}|$ of the ultrathin hybrid metamaterial when put the L-shaped particle in the corresponding position. The distribution of the x-polarized electric field magnitude is the function of the positon z induced by the polarization-dependent reflection of the nanoantenna array (see also Fig. 3d). Therefore, the $|T_{yx}|$ of the ultrathin hybrid metamaterial will periodically vary with the changing of the distance between the L-shaped particle and the nanoantenna array. If the L-shaped particle is placed at the position of the maximal electric field magnitude, the $|T_{yx}|$ can be enhanced about two times larger than that of the solitary L-shaped particle. According to Eq. 7, the y-polarized transmitted intensity of the ultrathin hybrid metamaterial will further enhance about four times for fixed incident intensity. Figure 4b gives the normalized electric field distribution $|E_x|/|E_0|$ of the solitary nanoantenna array and the $|T_{yx}|$ of the ultrathin hybrid metamaterial for the different wavelengths when the L-shaped particle is located at 300 nm in -z direction (the position of maximal electric field magnitude at the incident wavelength of 1400 nm). Results show that the polarization conversion effect can be enhanced in a broadband wavelength range.To further show the enhancement of the polarization conversion efficiency of the L-shaped particle by its surrounding electric field, we plotted the maps of the electric field intensity components on the surface of L-shaped particle in x-y plane normalized by the incident electric field intensity $|E_0|$

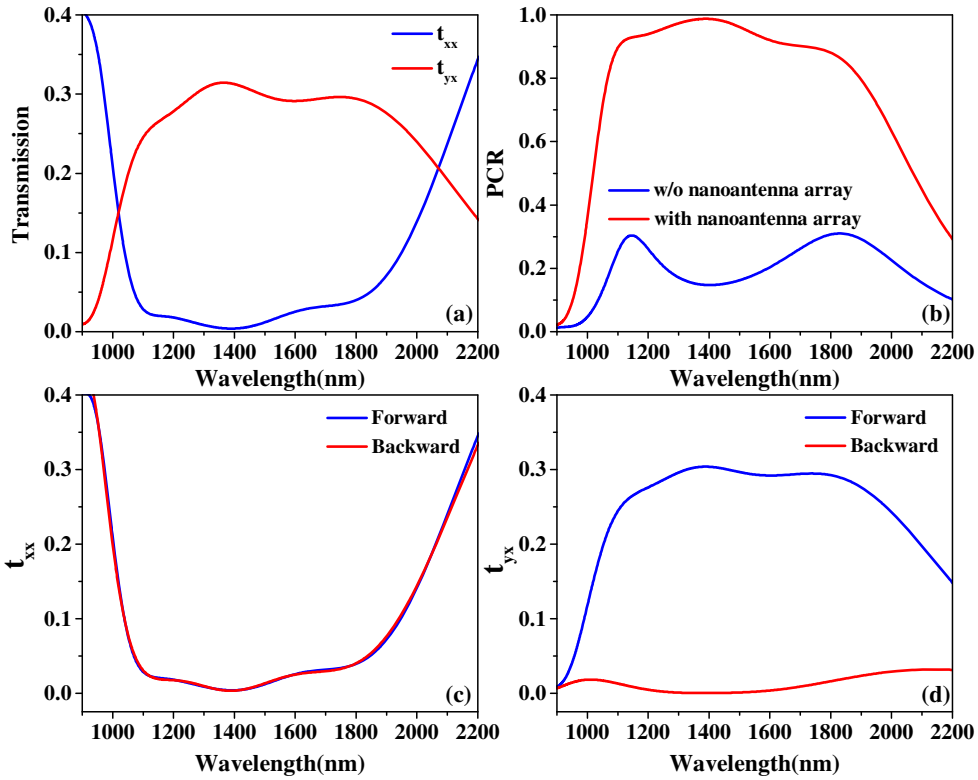

Fig. 6 **a** Calculated polarized transmittances t_{xx} and t_{yx} of the ultrathin hybrid, **b** PCR of the ultrathin hybrid metamaterial and the solitary L-shaped particle; **c** t_{xx} and **d** t_{yx} of the ultrathin hybrid for both forward and backward propagation

for solitary L-shaped particle and ultrathin hybrid metamaterial in Fig. 5, where the incident wavelength is 1400 nm. It is obvious that the oscillating mode of the electron is not changed for two cases. Otherwise, the oscillation intensity of the electron is apparently enhanced.

A broadband and high efficiency polarization conversion can be thereby achieved by the enhancement of electric field. The polarized transmittances t_{xx} and t_{yx} of the ultrathin hybrid as a function of wavelength are shown in Fig. 6a. The t_{yx} is enhanced by the electric field distribution formed by the x-polarized incident and reflected wave and the t_{xx} is eliminated by the polarization-dependent reflection of the nanoantenna array. Consequently, a high performance polarization conversion on a 1000-nm-wide band at wavelength 1000–2000 nm is realized. The polarization conversion efficiency of the ultrathin hybrid metamaterial is accordingly enhanced compared with that of the solitary L-shaped particle, as shown in Fig. 6b. Moreover, the asymmetric polarization conversion can also be achieved by the polarization-dependent reflection of the nanoantenna array. The t_{xx} and t_{yx} for both forward and backward propagation as a function of wavelength are given in Fig. 6c, d, respectively. Results show that x-polarized wave will be transmitted into the opposite polarization for forward propagation and completely reflects for backward propagation. Menzel et al. proposed L-shaped and striped particles to achieve a narrowband asymmetric transmission for linearly polarized light in the near-infrared [26], which is mainly caused by three-dimensional chirality and complex resonances between the L-shaped and striped particles. Our proposed broadband asymmetric polarization conversion of linearly polarized light is formed by the broadband polarization-dependent reflection of the nanoantenna array.

In reality, the dielectric spacer and substrate needs to be taken into account for the practical realization of the metamaterials. By adding a silicon dioxide with relative refractive index of 1.47, the inclusion resonance will shift to longer wavelengths [9], so the optimal design needs to take into account its influence. The effective wavelength band of the nanoantenna array and the L-shaped particle will be changed. The position z of the L-shaped particle also needs to be varied to enhance the magnitude of the electric field in the effective wavelength band range. Figure 7 shows how the previous results are affected by such a glass spacer and substrate by keeping the design unchanged. It is observed that the broadband polarization conversion effect is shifted to the longer wavelength. Furthermore, the t_{xx} is almost 0 for the proposed ultrathin hybrid metamaterial with the dielectric for its inherent losses, which means the

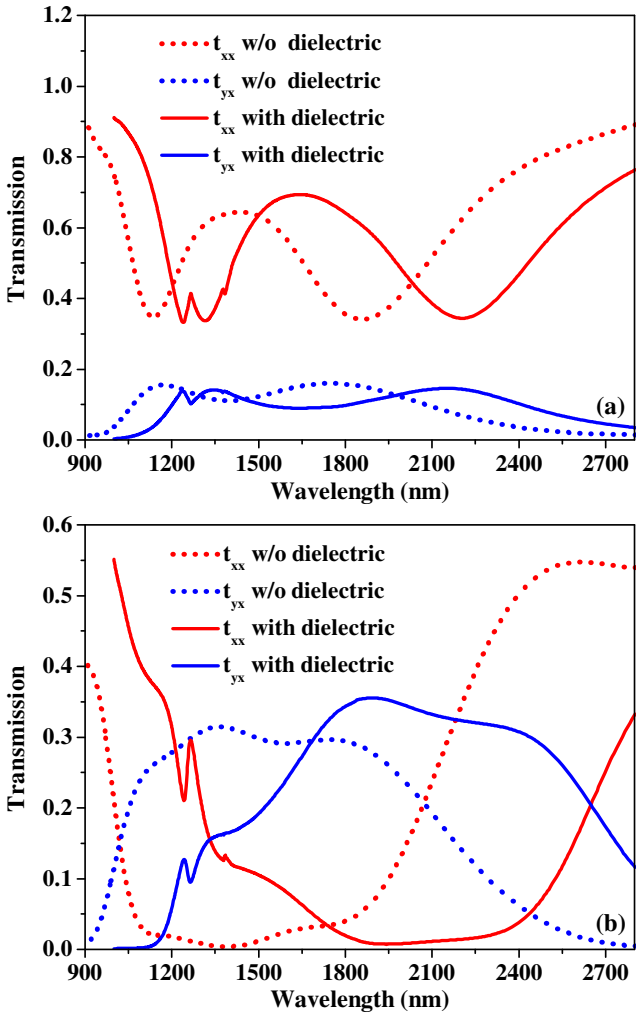

Fig. 7 Comparison of the polarized transmittances with and without dielectric for **a** the solitary L-shaped particle and **b** the ultrathin hybrid metamaterial

polarization of transmission wave is entirely changed to y direction. Obviously, a new design considering the presence of dielectric may further improve the overall functionality by optimizing the structure parameters of the ultrathin hybrid metamaterial. Considering the shift of the inclusion resonance caused by the dielectric spacer and substrate, a high performance polarization conversion with a 1000 nm bandwidth at the range of 1000–2000 nm can still be realized by optimizing the parameters of the ultrathin hybrid metamaterial with: $P = 500$ nm, $L_1 = 290$ nm, $W_1 = 100$ nm, $L_2 = 300$ nm , $L_3 = 370$ nm, $W_2 = 50$ nm, $W_3 = 50$ nm, $s = 50$ nm, $t_1 = 30$ nm, and $t_2 = 250$ nm. Moreover, the practical fabrication of such ultrathin hybrid metamaterial can be realized by using electron-beam lithography, evaporation deposition of gold, and plasma-enhanced chemical vapor deposition of silicon dioxide [24].

Conclusion

In conclusion, we have proposed an ultrathin hybrid metamaterial that is composed of an L-shaped gold particle and a gold nanoantenna array. The broadband polarization-dependent reflection of the nanoantenna array effectively enhances the polarization conversion efficiency. As a result, a broadband (1000–2000 nm) and almost complete (PCR>95 %) asymmetric polarization conversion is realized. To some extent, this approach of broadband polarization-dependent reflection provides a new way to improve the performance of the polarization conversion. This result offers helpful insight, and provides intriguing possibilities to the design of devices based on asymmetric polarization conversion.

Acknowledgments This work was supported by the National Basic Research Program (973 Program) of China (2012CB921900), the Chinese National Key Basic Research Special Fund (2011CB922003), the Natural Science Foundation of China (61378006 and 11304163), the Program for New Century Excellent Talents in University (NCET-13-0294), the International Science & Technology Cooperation Program of China (2013DFA51430), the Specialized Research Fund for the Doctoral Program of Higher Education (20120031120032), the Natural Science Foundation of Tianjin (13JCQNJC01900), the National Science Fund for Talent Training in Basic Sciences (J1103208), and the 111 project (B07013).

References

1. Li J, Chen S, Yang H, Li J, Yu P, Cheng H, Gu C, Chen H-T, Tian J (2015) Simultaneous control of light polarization and phase distributions using plasmonic metasurfaces. Adv Funct Mater 25:704
2. Huang C-P, Wang Q-J, Yin X-G, Zhang Y, Li J-Q, Zhu Y-Y (2014) Break through the limitation of malus law with plasmonic polarizers. Adv Opt Mater 2:723–728
3. Hao J, Yuan Y, Ran L, Jiang T, Kong JA, Chan CT, Zhou L (2007) Manipulating electromagnetic wave polarizations by anisotropic metamaterials. Phys Rev Lett 063908:99
4. Ye Y, He S (2010) 90° polarization rotator using a bilayered chiral metamaterial with giant optical activity. Appl Phys Lett 96:203501
5. Mutlu M, Akosman AE, Serebryannikov AE, Ozbay E (2011) Asymmetric chiral metamaterial circular polarizer based on four U-shaped split ring resonators. Opt Lett 36:1653–1655
6. Li T, Wang SM, Cao JX, Liu H, Zhu SN (2010) Cavity-involved plasmonic metamaterial for optical polarization conversion. Appl Phys Lett 261113:97
7. Wu S, Zhang Z, Zhang Y, Zhang KY, Zhou L, Zhang XJ, Zhu YY (2013) Enhanced rotation of the polarization of a light beam transmitted through a silver film with an array of perforated S-shaped holes. Phys Rev Lett 207401:110
8. Cheng H, Chen S, Yu P, Li J, Xie B, Li Z, Tian J (2013) Dynamically tunable broadband mid-infrared cross polarization converter based on graphene metamaterial. Appl Phys Lett 223102:103
9. Zhao Y, Alú A (2011) Manipulating light polarization with ultrathin plasmonic metasurfaces. Phys Rev B 205428:84

10. Zhao Y, Alú A (2013) Tailoring the dispersion of plasmonic nanorods to realize broadband optical meta-wave plates. Nano Lett 13:1086–1091
11. Wei Z, Cao Y, Fan Y, Yu X, Li H (2011) Broadband polarization transformation via enhanced asymmetric transmission through arrays of twisted complementary split-ring resonators. Appl Phys Lett 99:221907
12. Jiang SC, Xiong X, Hu YS, Hu YH, Ma GB, Peng RW, Sun C, Wang M (2014) Controlling the polarization state of light with a dispersion-free metastructure. Phys Rev X 4:021026
13. Grady NK, Heyes JE, Chowdhury DR, Zeng Y, Reiten MT, Azad AK, Taylor AJ, Dalvit DAR, Chen H-T (2013) Terahertz metamaterials for linear polarization conversion and anomalous refraction. Science 340:1304–1307
14. Lévesque Q, Makhsiyan M, Bouchon P, Pardo F, Jaeck J, Bardou N, Dupuis C, Haïdar R, Pelouard JL (2014) Plasmonic planar antenna for wideband and efficient linear polarization conversion. Appl Phys Lett 111105:104
15. Wu C, Li H, Yu X, Li F, Chen H, Chan CT (2011) Metallic helix array as a broadband wave plate. Phys Rev Lett 177401:107
16. Zhao Y, Belkin MA, Alú A (2012) Twisted optical metamaterials for planarized ultrathin broadband circular polarizers. Nat Commun 3:870
17. Singh R, Plum E, Zhang W, Zheludev NI (2010) Highly tunable optical activity in planar achiral terahertz metamaterials. Opt Express 18:13425–13430
18. Sieber PE, Werner DH (2014) Infrared broadband quarter-wave and half-wave plates synthesized from anisotropic Bézier metasurfaces. Opt Express 22:32371–32383
19. Fedotov VA, Mladyonov PL, Prosvirnin SL, Rogacheva AV, Chen Y, Zheludev NI (2006) Asymmetric propagation of electromagnetic waves through a planar chiral structure. Phys Rev Lett 167401:97
20. Drezet A, Genet C, Laluet JY, Ebbesen TW (2008) Optical chirality without optical activity: How surface plasmons give a twist to light. Opt Express 16:12559–12570
21. CST Studio Suite Version (2013) Computer Simulation Technology AG, Darmstadt, Germany, 2013
22. Ordal MA, Long LL, Bell RJ, Bell SE, Bell RR, Alexander RWJr, Ward CA (1983) Optical properties of the metals Al, Co, Cu, Au, Fe, Pb, Ni, Pd, Pt, Ag, Ti, and W in the infrared and far infrared. Appl Opt 22:1099–1119
23. Zhang S, Fan WJ, Malloy KJ, Brueck SRJ, Panoiu NC, Osgood RM (2006) Demonstration of metal-dielectric negative-index metamaterials with improved performance at optical frequencies. J Opt Soc Am B 23:434–438
24. Li Z, Chen S, Tang C, Liu W, Cheng H, Liu Z, Li J, Yu P, Xie B, Liu Z, Li J, Tian J (2014) Broadband diodelike asymmetric transmission of linearly polarized light in ultrathin hybrid metamaterial. Appl Phys Lett 201103:105
25. Esfandyarpour M, Garnett EC, Cui Y, McGehee MD, Brongersma ML (2014) Metamaterial mirrors in optoelectronic devices. Nat Nanotechnol 9:542–547
26. Menzel C, Helgert C, Rockstuhl C, Kley EB, Tunnermann A, Pertsch T, Lederer F (2010) Asymmetric transmission of linearly polarized light at optical metamaterials. Phys Rev Lett 253902:104